ACTA ECOLOGICA SINICA
Volume 28, Issue 2, February 2008
Online English edition of the Chinese language journal

Available online at www.sciencedirect.com
ScienceDirect

Cite this article as: Acta Ecologica Sinica, 2008, 28(2), 627−635.

RESEARCH PAPER

Monitoring sandy desertification of Otindag Sandy Land based on multi-date remote sensing images

Liu Haijiang[1,2], Zhou Chenghu[1,*], Cheng Weiming[1], Long En[1], Li Rui[1,3]

1 *State Key Laboratory of Resources and Environmental Information System, Institute of Geographic Sciences and Natural Resources Research, Chinese Academy of Sciences, Beijing 100101, China*
2 *Graduate School of the Chinese Academy of Sciences, Beijing 100039, China*
3 *Information Engineering University of People's Liberation Army, Zhengzhou 450052, China*

Abstract: Sandy desertification is now the main ecological problem in the Otindag Sandy Land. In order to reveal the process of land degradation, especially the latest situation of sandy desertification, a method integrating remote sensing, Geographic Information System (GIS) and field survey was employed to build a sandy desertification dataset for analysis. Remote sensing images included the Landsat Thematic Mapper (TM) image in 1987, the Enhanced Thematic Mapper Plus (ETM^+) image in 2000, and the image with the Charge-Coupled Device Camera (CCD) on the China-Brazil Earth Resources Satellite (CBERS) in 2006. Five land-cover classes, including active sand dunes, fixed sand dunes, semi-fixed sand dunes, inter-dune grassland and wetlands, were identified. Results showed that the Otindag Sandy Land has been suffering sandy desertification since 1987 with 2 different desertified stages. The first stage from 1987 to 2000 was a severe sandy desertification period, characterized by the fixed sand dunes decreasing at a high speed, and the semi-fixed and active sand dunes increasing remarkably. The second stage spanned from 2000 to 2006 and the sandy desertification was weakened greatly. Although a large area of fixed sand dunes were transformed to other types, fixed sand dunes were still the dominant type in the Ointdag region at 2006. Spatial change detection based on active sand dunes showed that the expansion area was much larger than the reversion area in the past two decades, and that several active sand belts had been formed, suggesting that sandy desertification controlling of the Otindag Sandy Land will be a long-term task.

Key Words: Otindag Sandy Land; sandy desertification; CBERS; remote sensing; change detection

Sandy desertification is one of the main forms of land degradation in China, especially in northern China[1], which has kept expanding since the 1950's and has exerted severe impacts on regional socio-economic development and environmental security[2]. Harsh physiographic conditions (sparse vegetation coverage, sandy soil and water deficiency), irrational land-use practice and population augmentation are regarded as the forces of triggering sandy desertification[3,4]. Therefore, the sandy desertification assessment and monitoring are always concerned by researchers, the public and the policy-makers.

The Otindag Sandy Land, one of the 4 largest sandy lands in China, has suffered severe sandy desertification in the past decades[3,5,6]. The degraded land augmented 492 km^2/a from the 1950s to the mid-1970s, 205 km^2/a from the mid-1970s to the mid-1990s, and 2015 km^2/a from the mid-1990s to 2000[5]. This region has been thought as a source of sandy dust storm[7,8]. Therefore, it is quite necessary to monitor the sandy desertification of this region.

The major objective of this study is to assess the sandy desertification process of the Otindag Sandy Land in the past decades. A method of integrating remote sensing, geographic information system (GIS) and field survey was employed to generate a sandy desertification dataset of this region. Then change detection and land degradation process were performed based on the dataset. This study intends to provide useful information for sandy desertification controlling and environmental management of the Otindag area.

1 Study area

Received date: 2007-07-06; Accepted date: 2007-11-28
*Corresponding author. E-mail: zhouch@lreis.ac.cn

The Otindag Sandy Land (42°10′–43°50′N, 112°10′–116°30′E) is located in the southeastern part of Inner Mongolia[9] (Fig. 1), which is about 340 km in length from east to west and 30–100 km in width. The elevation varies between 1400 m and 1100 m and the topography declines from southeast to northwest. The climate is of temperate continental semi-arid type with strong wind and less precipitation in winter and spring. Annual average precipitation, mainly occurring in summer and fall with some inter-annual fluctuation, is nearly 400 mm in the southeastern part and below 200 mm in the northwest part[10,11]. The dominant vegetation is *Stipa grandis* and *Leymus chinensis* steppe. However, because of sandy substrate, the Otindag Sandy Land possesses a high degree of biodiversity and spatial heterogeneity. The notable landscape is of open forest steppe dominated by *Ulmus pumila*[12].

2 Data and methods

2.1 Data and pre-processing

Remote sensing images used in this study include the Landsat5 Thematic Mapper (TM) image, the Landsat7 Enhanced Thematic Mapper Plus (ETM^+) image, and the image with the Charge-Coupled Device Camera (CCD) on the China- Brazil Earth Resources Satellite (CBERS), which were acquired in 1987, 2000 and 2006, respectively (Table 1). The ETM^+ images were acquired eventually in 1999, 2000 and 2001, hereafter named as the 2000 data. The CBERS was jointly developed by China and Brazil since 1988, who planned to launch a series of satellites used for resources and environmental monitoring. Two satellites (CBERS-1,2) were launched in October of 1999 (CBERS-1) and 2003 (CBERS- 2), respectively. CCD is one of the 3 sensors loaded on CBERS, which has a nadir spatial resolution of 19.5 m, swath width of 113 km and 5 spectral bands including blue (0.45– 0.52 μm), green (0.52–0.59 μm), red (0.63–0.69 μm), near infrared (0.77–0.89 μm) and panchromatic band (0.51–0.73 μm). More information can be found at the website of the China Center for Resources Satellite Data and Applications (CRESDA) at http://www.cresda.com.cn/. All these data have been processed to level 2 by a data supply agency, namely, systematic geometric correction and radiometric calibration were performed. Here, they are geo-referenced to the Albers Equal-area Conic coordinate system by using ground control points (GCP) based on 1:100000 scale topographic maps, and the root mean square error was less than one pixel.

In order to remove or normalize the reflectance variation between images acquired at different times, relative radiometric correction was performed to yield normalized radiometric data on a common scale[13]. Here, the histogram normalization, a simpler and more effective technique, was used to carry out the relative radiometric correction[14]. As for the Landsat images, the 2000 data were used for master images to correct those in 1987, whereas the CCD data were calibrated among

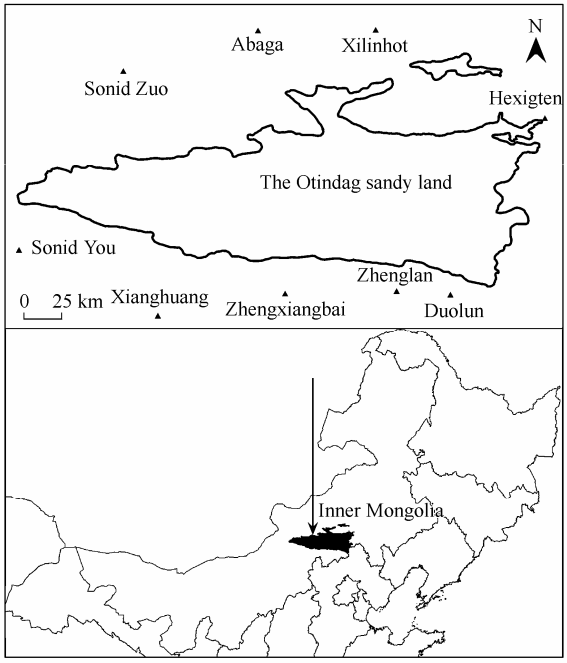

Fig. 1 Location of the Otindag Sandy Land

Table 1 Characteristics of remote sensing images used in this study

Scene's ID (Path/row)	Acquired time (year/month/day)	Sensor type
123/30	1987/09/10	TM
	2001/07/06	ETM^+
124/30	1987/07/31	TM
	2000/07/10	ETM^+
125/30	1987/10/27	TM
	1999/07/23	ETM^+
126/30	1987/06/27	TM
	1999/09/24	ETM^+
001/051,052,053	2006/09/06	CCD
002/051,052	2006/07/13	CCD
003/051,052	2006/08/31	CCD
004/051,052	2006/09/23	CCD
005/051,052	2006/07/30	CCD
006/051,052	2006/07/27	CCD

paths, and the 003 path, which had the best quality through visual inspection, was used to match with the others. The near infrared, red and green bands were superimposed into false-color images for different scenes in the same path, which were set together, and then path-to-path histogram normalization was performed.

2.2 Spectral transformation of Landsat images

Spectral transformation can reduce multi-spectral data volume with minimal information loss and generate a new image which loads main information of original data. It is an effective technique in improving classification accuracy and change

detection[16]. The Tasseled Cap transformation, also called as K-T transformation and originally applied to the Landsat Multispectral Scanner (MSS) data, is a principal component analysis technique, which linearly transforms multi-spectral data and creates 3 uncorrelated bands: Brightness (B), Greenness (G) and Wetness (W)[15–17]. The Tasseled Cap transformation is scene independent and has fixed coefficients, and therefore the multi-date TM and ETM^+ data can be transformed through this technique and the results are comparable over time. The BGW bands are directly related to specific physical attributes and can be easily interpreted. Brightness can be interpreted as change in total reflectance or albedo at the surface, and is mainly driven by soil reflectance variations; Greenness measures the contrast between visible bands and near infrared band, and has a close correlation with vegetation coverage, just like the vegetation index; Wetness is sensitive to soil and plant moisture[17]. After transformation, the BGW bands were combined into a new image.

2.3 Generating sandy desertification dataset

2.3.1 Class definition

Vegetation coverage is the most remarkable symbol to reflect sandy desertification situation[3]. Several land cover types were identified according to vegetation coverage; meanwhile, species composition and structure of plant community were also considered. They are active sand dunes, fixed sand dunes and semi-fixed sand dunes, which not only reflect ecological conditions that are important to environment management and resource utility but are also distinguishable in remote sensing images. Active sand dunes, the most severely degraded type, are dominated by psammophytes and annual pioneer plants with high surface reflectance and lower greenness on images, and vegetation coverage is less than 20%. Semi-fixed sand dunes, a transitional type, have vegetation coverage from 20% to 50%, and are transformed from fixed sand dunes or active sand dunes. Fixed sand dunes have dense vegetation with coverage more than 50% and a high biodiversity, with high greenness and low brightness on images. In addition, 2 other classes, wetlands and inter-dune grassland, are also identified. Inter-dune grassland, mainly distributed in the eastern part of the Otindag Sandy Land, occurs in flat, undulated plains between sand dunes and has high resistance to disturbance. Inter-dune grassland can be used as mowing pasture and can be cultivated. Wetlands, including water body, swamp and dense bushwood, are water source for livestock and shelters for wild animals. Characteristics of the 5 classes were determined by field survey and remote sensing images.

Field work was carried out in July 2001 and August 2006, and data of 121 and 209 sample sites were collected, respectively. At each site, the structure and species composition of plant communities, projected vegetation coverage, and soil features were recorded; meanwhile, the location was positioned by the portable Global Positioning System (GPS) receiver. These sample points covered the entire Otindag Sandy Land and were digitized into the images according to their geographic position.

2.3.2 Supervised classification and dataset building

Training pixels were selected for each class on images, and the maximum likelihood classification was carried out in ERDAS IMAGINE8.7 to derive the thematic maps of 1987, 2000 and 2006. After the post-classification process, the accuracy assessment was performed. The 2000 and 2006 classified maps were assessed by field survey data, all the points were employed to evaluate classification accuracy, *i.e.*, 121 points in 2000 and 209 points in 2006. Error matrix was derived and the overall accuracy reached 89.25% and 92.34%, respectively. Because no appropriate reference data were available for assessing 1987 classified map, we used the 2000 classified map as reference data to evaluate 1987 classified map. 150 points were randomly selected, and the overall accuracy was 87.33%, indicating that all the maps were acceptable[18].

The 3 classification maps were subset to the boundary of the Otindag Sandy Land which was delimited by experts in aeolian landform according to remote sensing images in 2000, and then these classified raster maps were converted to maps of ArcGIS vector format. The patches of different classes in classified maps were represented as polygons in ArcGIS which were enclosed by a group of lines connected with each other. Visual inspection was conducted through superimposing the field survey points, remote sensing images and vector sandy desertification data together to correct some misclassified classes, and then sandy desertification dataset was built up (Fig. 2).

2.4 Change detection

In order to reveal the sandy desertification process in the Otindag area, change detection was carried out based on active sand dunes in 1987, 2000 and 2006 because the active sand dunes can be used as an indicator of sandy desertification situation. At first, 5 classes were regrouped into active sand dunes and non-active sand dunes, and then the dataset was converted into ArcGIS raster format—GRID with coded binary values 0 (non-active sand dunes) and 1 (active sand dunes). The pixel size is 30 m. The binary GRIDs of 1987, 2000 and 2006 were combined together to generate a new GRID with 2^3 different outcomes including 000, 010, 100, 110, 011, 001, 101 and 111 (Fig. 3). The figure per outcome was arranged in the time order. For example, 101 indicates that a pixel was active sand dunes in 1987, non-active sand dunes in 2000 and returned to active sand dunes in 2006. So every outcome implied one kind of change trajectory of active sand dunes.

According to the change trajectory of active sand dunes, the 8 outcomes were grouped into 4 classes named as inactivation, reversion, deterioration and no change. The inactivation type, including 000, meant that pixels kept non-active sand dunes

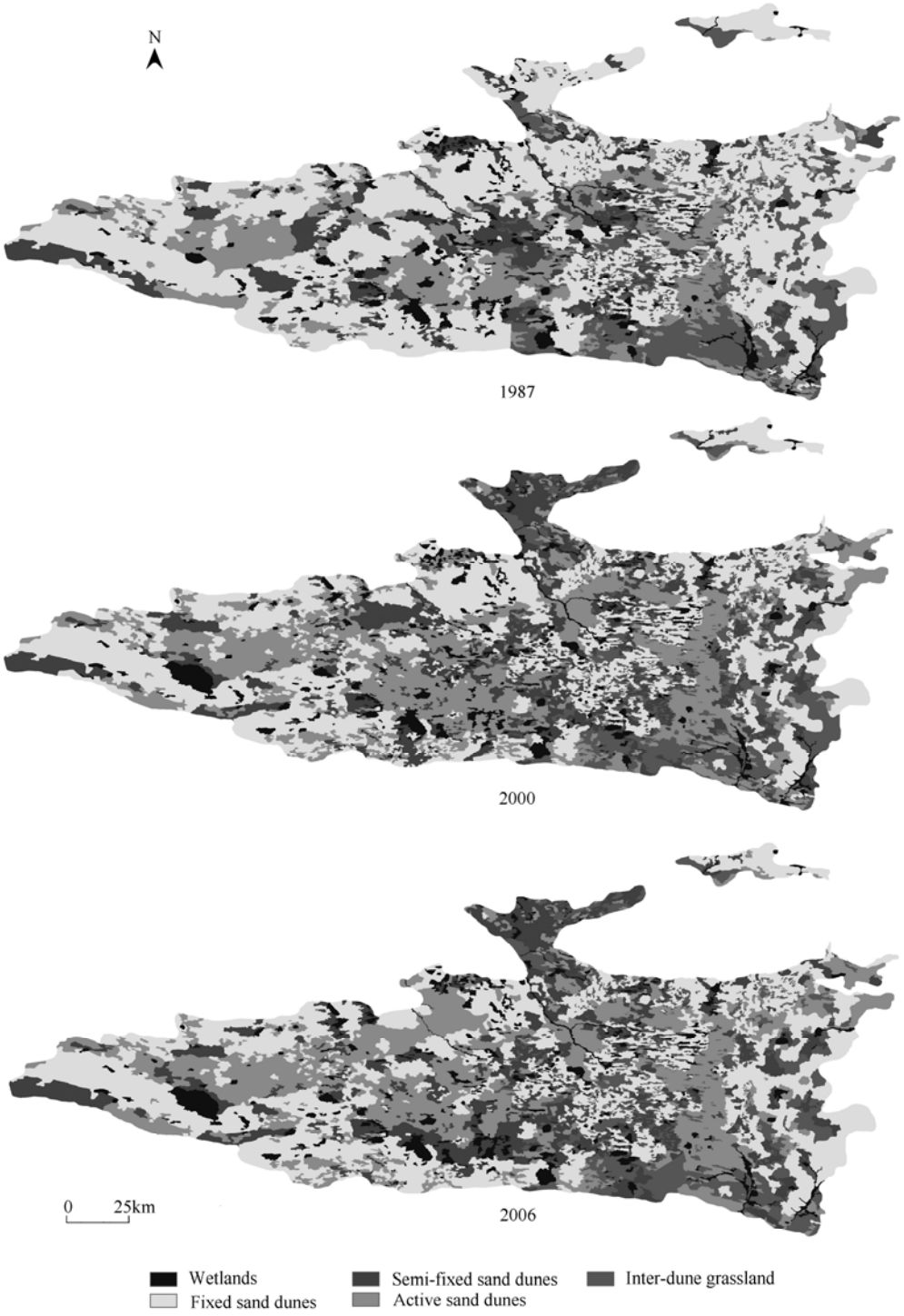

Fig. 2 Maps of sandy desertification in the Otindag Sandy Land in 1987, 2000 and 2006

from 1987 to 2006. Reversion type, including 010, 100 and 110, implied that pixels were active sand dunes in 1987 or 2000, and converted to non-active sand dunes in 2006. Deterioration type, containing 011, 001 and 101, was just opposite to the reversion type, which meant that pixels belonged to non-active sand dunes in 1987 or 2000, and transformed to active sand dunes in 2006. No change class, including 111, meant that pixels retained active sand dunes from 1987 to 2006.

3 Results

3.1 Sandy desertification processes

Remarkable ecological change occurred in the Otindag

Sandy Land in the past decades. From 1987 to 2006, the fixed sand dunes, which covered half area (14570.93 km^2; 50.25%) in 1987, sharply shrank to 10608.96 km^2 (36.6%) in 2000 with a decreasing rate of 304.77 km^2/a. The semi-fixed sand dunes, however, increased from 3405.41 km^2 (11.70%) in 1987 to 4911.13 km^2 (16.94%) in 2000 with a growth rate of 115.82 km^2/a. The active sand dunes, following the same trend as the semi-fixed sand dunes, increased to 8090.70 km^2 (27.91%) in 2000 with a change rate of 201.67 km^2/a. The inter-dune grassland decreased at a rate of 22.20 km^2/a, whereas wetlands increased slowly at an increasing rate of 9.47 km^2/a (Table 2 and Fig. 4).

In contrast, there were some differences in the land degradation process from 2000 to 2006, the second period. The noticeable change was the increase of fixed sand dunes with a rate of 30.31 km^2/a. The semi-fixed sand dunes and active sand dunes remained augmentation, but the increased magnitude was sharply declined. However, the inter-dune grassland reduced at a higher speed. Wetlands decreased with a speed of 7.18 km^2/a. Although the decrease in area was significant, the fixed sand dunes remained to be the largest area in the Otindag Sandy Land in 2006 (Table 2).

We can conclude from the results that the sandy desertification process of the Otindag Sandy Land can be divided into 2 different stages. The first stage, from 1987 to 2000, was characterized by the land degradation with a high speed, whereas the second stage, from 2000 to 2006, presented a notable alleviation of ecological deterioration.

3.2 Spatial change detection

Change detection could reveal the spatial dynamics of sandy desertification. As shown in Fig. 5, the 4 classes presented different patterns. Deterioration mainly occurred at periphery of no change class, namely, emergence of new active sand dunes was based on the old ones which kept active in the past two decades. Therefore, the patches of deterioration class and no change class were combined and formed several active sand belts (Fig. 5). Reversion class mainly covered the central-south part of the Otindag area.

Land degradation is the main ecological process in the Otindag area in the past two decades. Pixels of deterioration (4579057) and no change (4484457) were almost twice those of reversion (2303715). However, inactivation was still the dominant class which had the most pixels (20832938) among the 4 types (Table 3).

4 Discussion and conclusions

The Otindag Sandy Land became a hot spot because of the widespread sand storms in 2000. In this research, we employed the temporal remote sensing images to reveal the sandy desertification process in this region, especially the latest situation of sandy desertification.

Sandy desertification occurred in the Otindag Sandy Land in the past two decades from 1987 to 2006. The fixed sand dunes shrank, semi-fixed and active sand dunes increased remarkably; meanwhile, the inter-dune grassland and wetlands also decreased (Table 2; Figs. 4 and 5). Two different sandy desertification stages could be identified. From 1987 to 2000 (the first stage), land degradation proceeded at a higher speed,

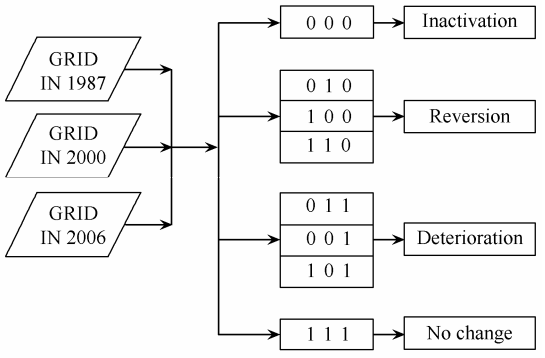

Fig. 3 Types of change detection

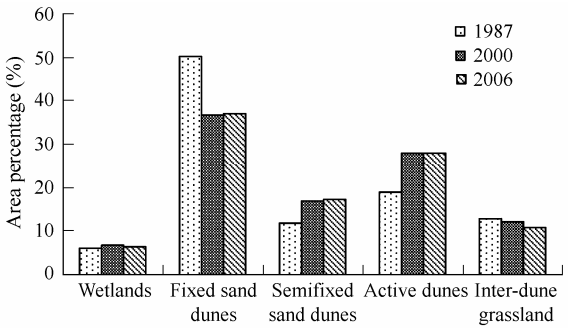

Fig. 4 Area percentage of the 5 land cover types in 1987, 2000 and 2006 in the Otindag area

Table 2 Change rate of the 5 land cover classes from 1987 to 2006 in the Otindag area

Land cover type	Area (km^2)			Change rate (km^2/a) (+Gain,−Loss)	
	1987	2000	2006	1987–2000	2000–2006
Fixed sand dunes	14570.93	10608.96	10790.84	−304.77	+30.31
Semi-fixed sand dunes	3405.41	4911.13	5039.75	+115.82	+21.44
Active sand dunes	5468.99	8090.70	8160.94	+201.67	+11.7
Inter-dune grassland	3761.75	3473.23	3135.59	−22.20	−56.27
Wetlands	1784.76	1907.86	1864.78	+9.47	−7.18

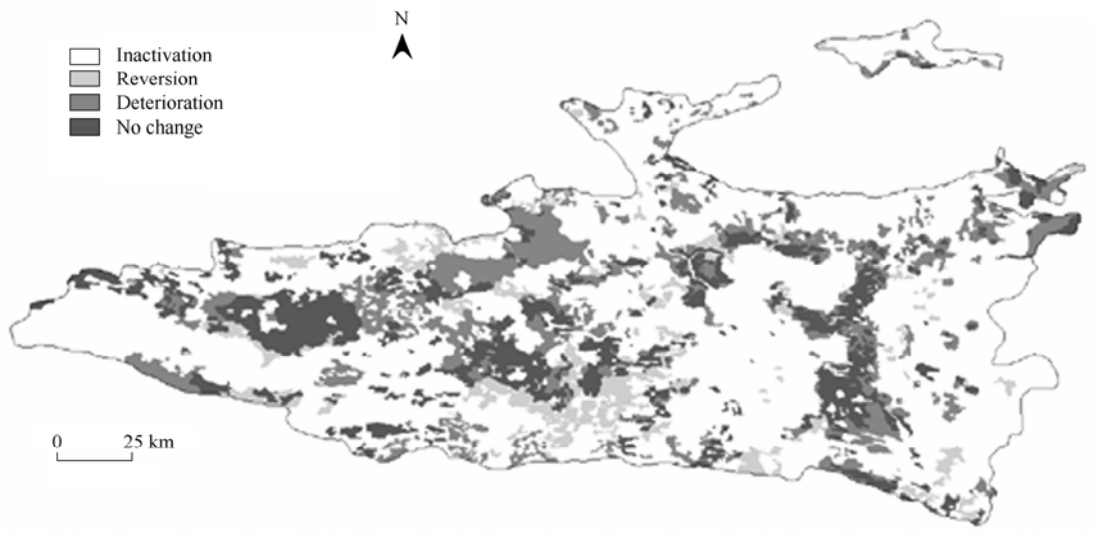

Fig. 5 Change detection of active sand dunes from 1987 to 2006 in the Otindag area

Table 3 Pixel number of the 4 change detection classes

Inactivation	Reversion	Deterioration	No change
20832938	2303715	4579057	4484457

whereas from 2000 to 2006 (the second stage), sandy desertification was greatly alleviated. Although severe land degradation occurred, the fixed sand dunes still dominated in the Otindag area in 2006. The spatial change detection showed that area of deterioration was much larger than that of reversion, and that several active sand belts had been formed (Table3 and Fig. 5).

Ecological deterioration of this region is mainly a human-induced process, and the climate did not have notable changes with only normal fluctuation[19–21]. In the past two decades, this region experienced rapid population increase. Life demand of local people caused overgrazing and reclamation on grassland to improve income. Meanwhile, no adequate attention was paid for protecting and restoring vegetation, which in consequence led to degradation of natural vegetation and triggered sandy desertification.

Policies have played an important role in controlling sandy desertification[22]. The alleviation of sandy desertification from 2000 to 2006 mainly resulted from a series of ecological restoration projects. In 2000, a nation-wide ecological restoration project, named as the Grain-for-Green Project, was launched and regulations were enacted by the central government. This project aims to reduce the cropland which is not suitable for cultivation so as to restore natural vegetation. The ultimate goal is to attain sustainable development of society, economy and environment. In the Otindag area, a series of measures, aimed at weakening the disturbance and increasing the coverage of natural vegetation, were taken by local governments to control further ecological degradation, which included grazing prohibition, plantation of high yield forage grasses, aerial seeding by planes, and adjustment of socio-economic structure. After several years' practice, the sandy desertification was greatly alleviated. From this research, we can suggest affirmatively that these measures were indeed effective in controlling land degradation. However, because long time is needed in the restoration of the damaged sandy ecosystem, the policies, made by decision-makers, will be valid in a longer time span.

Acknowledgements

This study was funded by National Natural Science Foundation of China (No. 40401048).

References

[1] Wang T, Zhu Z D. Studies on the sandy desertification in China. Chinese Journal of Eco-agriculture, 2001, 9(2): 7–12.

[2] Wang T, Chen G T, Zhao H L, *et al*. Research progress on aeolian desertification process and controlling in north of China. Journal of Desert Research, 2006, 26(4): 507–516.

[3] Zhu Z D, Chen G T. Sandy desertification in China. Beijing: Science Press, 1994. 20–33.

[4] Chen Y F, Tang H P. Desertification in north China: background, anthropogenic impacts and failures in combating it. Land Degradation and Development, 2005, 16: 367–376.

[5] Liu S L, Wang T. Primary study on sandy desertification in Otindag Sandy Land and its surrounding regions. Journal of Soil and Water Conservation, 2004, 18(5): 99–103.

[6] Fan J Y, Ding G D, Guan B Y, *et al*. Monitoring remote sensing of dynamic change of vegetation coverage in Zhenglan Banner. Science of Soil and Water Conservation, 2005, 3(4): 54–59.

[7] Wang T, Chen G T, Qian Z G, *et al*. The situation of dust

storms and its strategy in north China. Bulletin of the Chinese Academy of Sciences, 2001, 5: 343–348.

[8] Liu H Y, Tian Y H, Ding D. Contributions of different land cover types in Otindag Sandy Land and Bsshang region of Hebei Province to the material source of sand stormy weather in Beijing. Chinese Science Bulletin, 2003, 48(11): 1853–1856.

[9] Zhu Z D, Wu Z, Liu S. The generality of deserts in China. Beijing: Science Press, 1980. 80–107.

[10] Wang W H. Climate of Inner Mongolia. Beijing: China Meteorological Press, 1990. 183–188.

[11] Bai M L, Hao R Q, Di R Q, *et al.* Assessment of climatic variation impact on desertification of Otindag Sandland. Climatic and Environmental Research, 2006, 11(2): 215–220.

[12] Guo K, Liu H J. A comparative research on the development of elm seedlings in four habitats in the Hunshandak Sandland, Inner Mongolia. Acta Ecologica Sinica, 2004, 24(9): 2024–2028.

[13] Paolini L, Grings F, Sobrino J A, *et al*. Radiometric correction effects in Landsat multi- date/multi-sensor change detection studies. International Journal of Remote Sensing, 2006, 27: 685–704.

[14] Ding L X, Zhou B, Wang R C. Comparison of five relative radiometric normalization techniques for remote sensing monitoring. Journal of Zhejiang University (Agriculture and Life Sciences), 2005, 31(3): 269–276.

[15] Zhao Y S. Principles and methods in remote sensing application and analysis. Beijing: Science Press, 2003. 188– 190.

[16] Seto K C, Woodcock C E, Song C, *et al*. Monitoring land-use change in the Pearl River Delta using Landsat TM. International Journal of Remote Sensing, 2002, 23: 1985–2004.

[17] Masoud A A, Koike K. Arid land salinization detected by remotely-sensed landcover changes: A case study in the Siwa region, NW Egypt. Journal of Arid Environment, 2006, 66: 151–167.

[18] Congalton R G, Green K. Assessing the accuracy of remotely sensed data: principles and practices. Boca Raton, London, New York, Washington, D.C.: Lewis Publishers, 1999. 45–55.

[19] Li Q F, Hu C Y, Wang M J. Analysis on the causes of eco-environmental deterioration in Hunshandake Sandy land region and countermeasures. Journal of Arid Land Resources and Environment, 2001, 15(3): 9–16.

[20] Zheng Y R, Xie Z X, Robert C, *et al*. Did climate drive ecosystem change and induce desertification in Otindag Sandy Land, China over the past 40 years? Journal of Arid Environment, 2006, 64: 523–541.

[21] Liu S L, Wang T. Characteristic of climatic change in the Otindag Sandy Land region. Journal of Desert Resources, 2005, 25(4): 557–562.

[22] Oñate J J, Peco B. Policy impact on desertification: stakeholders' perception in southeast Spain. Land Use Policy, 2005, 22: 103–114.